Journal Pre-proofs

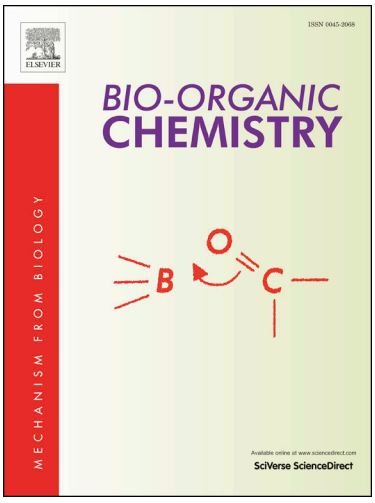

A Pt(IV)-based Mononitro-naphthalimide Conjugate with Minimized Side-effects Targeting DNA Damage Response via a Dual-DNA-Damage Approach to Overcome Cisplatin Resistance

Yingguang Li, Kexin Yue, Linrong Li, Jie Niu, Hanfang Liu, Jing Ma, Songqiang Xie

PII: S0045-2068(20)31308-0
DOI: https://doi.org/10.1016/j.bioorg.2020.104011
Reference: YBIOO 104011

To appear in: *Bioorganic Chemistry*

Received Date: 16 May 2020
Revised Date: 8 June 2020
Accepted Date: 10 June 2020

Please cite this article as: Y. Li, K. Yue, L. Li, J. Niu, H. Liu, J. Ma, S. Xie, A Pt(IV)-based Mononitro-naphthalimide Conjugate with Minimized Side-effects Targeting DNA Damage Response via a Dual-DNA-Damage Approach to Overcome Cisplatin Resistance, *Bioorganic Chemistry* (2020), doi: https://doi.org/10.1016/j.bioorg.2020.104011

A Pt(IV)-based Mononitro-naphthalimide Conjugate with Minimized Side-effects Targeting DNA Damage Response via a Dual-DNA-Damage Approach to Overcome Cisplatin Resistance

Yingguang Li,[a]# Kexin Yue,[a]# Linrong Li,[a]# Jie Niu,[a] Hanfang Liu,[a] Jing Ma,[a],* and Songqiang Xie,[a],*

[a] School of Pharmacy, Institute for Innovative Drug Design and Evaluation, Henan University, N. Jinming Ave, 475004 Kaifeng, China. # These authors have contributed equally to this work.

KEYWORDS: Pt Drugs, Mononitro-naphthalimide Conjugate, DNA Damage Repair, Dual DNA Damage Approach, Overcome Cisplatin Resistance

ABSTRACT: Platinum(Pt)(II) drugs and new Pt(IV) agents behave the dysregulation of apoptosis as the result of DNA damage repair and thus, are less effective in the treatment of resistant tumors. Herein, mononitro-naphthalimide Pt(IV) complex **10b** with minimized side-effects was reported targeting DNA damage response *via* a dual-DNA-damage approach to overcome cisplatin resistance. **10b** displayed remarkably evaluated antitumor (70.10%) activities *in vivo* compared to that of cisplatin (52.88%). The highest fold increase (FI) (5.08) for A549cisR cells and the lowest (0.72) for A549 indicated **10b** preferentially accumulated in resistant cell lines. The possible molecular mechanism indicates that **10b** targets resistant cells in a totally different way from the existing Pt drugs. The cell accumulation and the Pt levels in genomic DNA from **10b** is almost 5 folds higher than that of cisplatin and oxaliplatin, indicating the naphthalimide moiety in **10b** exhibits preferentially DNA damage. Using 5'-dGMP as a DNA model, the DNA-binding properties of **10b** (1 mM) with 5'-dGMP (3 mM) in the presence of ascorbic acid (5 mM) deduced that **10b** was generated by the combination of cisplatin with 5'-dGMP after reduction by ascorbic acid. Moreover, **10b** promoted the expression of p53 gene and protein more effectively than cisplatin, leading to the increased anticancer activity. The up-regulated γH2A.X and down-regulated RAD51 indicates that **10b** not only induced severe DNA damage but also inhibited the DNA damage repair, thus resulting in its higher cytotoxicity in comparison to that of cisplatin. Their preferential accumulation in cancer cells (SMMC-7721) compared to the matched normal cells (HL-7702 cells) demonstrated that they were potentially safe for clinical therapeutic use. In addition, the higher therapeutic indices of **10b** for 4T1 cells *in vivo* indicated that naphthalimide-Pt(IV) conjugates behaved a vital function in the treatment of breast cancer. For the first time, our study implies a significant strategy for Pt drugs to treat resistance cancer targeting DNA damage repair via dual DNA damage mechanism in a totally new field.

1. INTRODUCTION

FDA-approved the classical DNA-targeted drugs, cisplatin (CDDP), carboplatin and oxaliplatin, play important roles in treating a variety of cancers in clinics. [1] However, the Pt(II) drugs are clinically restricted by low DNA binding ratios, 85% - 90% of which cannot bind to DNA due to many factors including DNA damage response (DDR). Only less than 10% of Pt can bind with DNA to treat patients, especially in cisplatin-resistant cancer cells. [1b] The accumulation of Pt in healthy tissue leads to undesired side effects, including nephrotoxicity, peripheral neuropathy and nausea. [1-2] DDR also plays crucial roles in regulating the efficacy and drug resistance of anticancer drugs, especially Pt drugs, that exerts cytotoxicity through DNA damage. [3] Defects in DDR are one of the most pervasive characteristics of human cancer, allowing cancer cells to survive and proliferate. Very recently, small molecules targeting different DDR pathways have been used alone or in combination with radiation therapy and genotoxic chemotherapy for cancer treatment. [4]

In the past decade, Pt(IV) prodrugs, derived from the fusion of tumour targeting molecules and oxoplatin, have been developed to overcome the limitations existing in Pt(II)-based chemotherapies and attract substantial attention as the next generation of Pt-based candidates. [5] The special kinetically inertness of Pt(IV) compounds can avoid the reactions with off-target biological substances before attacking DNA. [6] Most importantly, our laboratories [7] or others [8] focused on the modification of two hydroxyl groups at axial positions of Pt(IV) drugs by introducing functional groups, such as prodrug activation, tumour targeting, or drug delivery to reduce the undesired side-effects and overcome cisplatin resistance. However, Pt(II) drugs and new Pt(IV) agents, which are widely used in the treatment of cancers in clinic, are less effective in the treatment of DDR. [8a] Novel strategies for chemother-

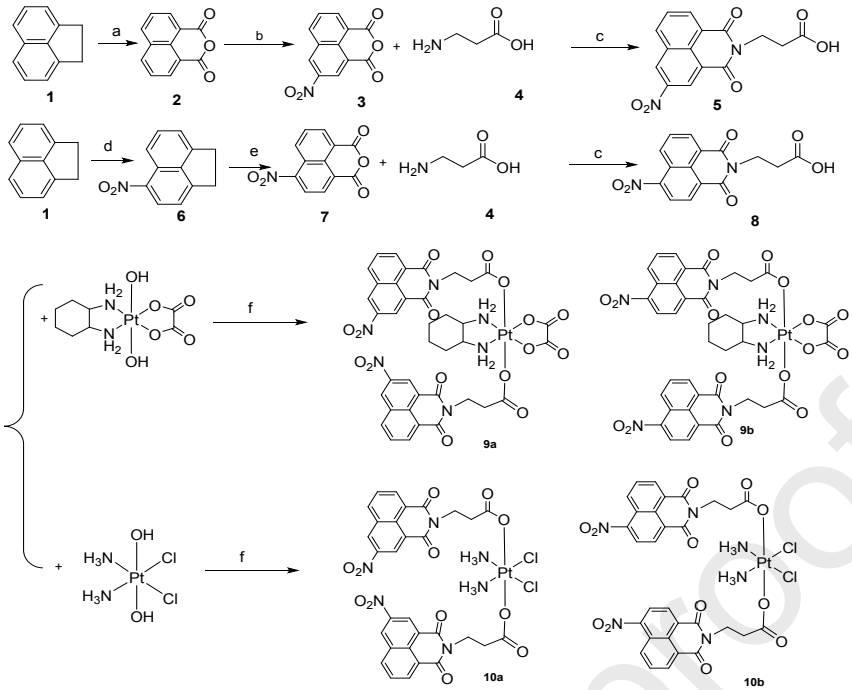

Scheme 1. Chemical structures and synthetic route of naphthalimide conjugates **9a-9b**, **10a-10b** in yield of 25%-30%. Reagents and conditions: (a) HNO_3, 50 °C, 3 h; (b) concH_2SO_4， conc HNO_3, 0 ℃; (c) K_2CO_3, CH_3CN, 85 °C , 5 h; (d) concHNO_3， AcOH, 0 ℃; (e) $Na_2Cr_2O_7$, AcOH, 100 ℃; (f) TBTU, DIPEA, rt, overnight.

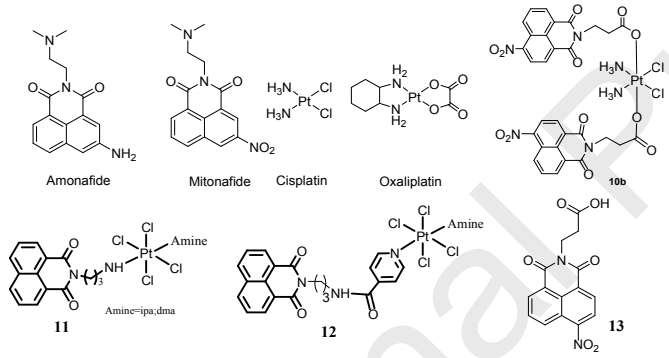

Figure 1. Chemical structures of amonafide, mitonafide, cisplatin, oxaliplatin, Pt(IV) complex **10b**, **11** , **12** and the released naphthalimide ligand **13**.

apeutic agents including Pt drug candidates are therefore of great interest to design novel therapeutic agents to target DDR with dual DNA damage mechanism to overcome cisplatin resistance. The relevant mechanism also need urgent attention. [8b]

Naphthalimides, a versatile functional compounds with large π -conjugated system, possess potential antitumor activities and photophysical characters *via* DNA damage by intercalation with DNA double helix. [9] Recently, naphthalimide was incorporated into platinum(IV) system to yield compounds **11** and **12** (Figure 1). [10] Our group also found crucial evidences that some naphthalimides conjugates, such as amonafide in clinic and mitonafide in Phase II clinical trials (Figure 1), could potently inhibit tumour growth and metastasis [11] *in vitro* and *in vivo*. Moreover, as a "carrier" of drugs, naphthalimide can remarkably increase their DNA targeting and influence the activities. Accordingly, naphthalimide as a DNA targeting fragment is of great potential in improving antitumor properties of platinum(IV) complexes. Moreover, natural products with a naphthalimides moiety have been found to be an effective methods to target DDR. γH2A.X [12-13] and RAD51 [14] play essential roles in HR (homologous recombination), which is a major way to repair the DNA double-strand breaks (DSBs) triggered by cisplatin. And RAD51 proficient tumours are usually refractory to cisplatin due to effective HR. However, little efforts have been put forward to design and investigate relevant mechanism of Pt(IV) conjugates with functionalized naphthalimides in targeting DNA damage repair derived from the RAD51 pathway *via* dual DNA damage mechanism to overcome cisplatin resistance.

In view of the facts mentioned above and in continuation of our ongoing interest in the development of new antitumor agents, [7, 11] for the first time, di-functionalized (**9a-9b**, **10a-10b**) Pt(IV) complexes were designed, which are multi-action Pt prodrugs with FDA-approved cisplatin and oxaliplatin cores, and the classical mitonafide analogues in Phase III clinical trials (Figure 1 and Scheme 1). [11] Feasible routes to **9a-9b**, **10a-10b** were established in Scheme 1.

Table 1. IC_{50} values (concentrations of 50% inhibition of cell proliferation) (micromolar) of Pt(IV) prodrugs. The cell viability was determined by MTT assays[a].

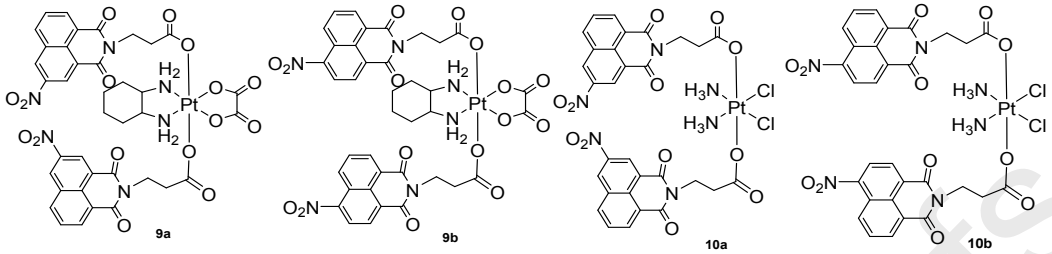

	HT-29	HCT-116	MDA-MB-231	MCF-7	4T1	A549cisR	A549	RF[b]
9a	14.72±1.47	14.72±1.47	19.35±0.73	11.73±0.29	ND	27.13 ± 1.95	41.20 ± 6.88	0.66
9b	12.72±1.67	12.72±1.67	15.35±1.93	6.45 ± 0.64	ND	17.13 ± 1.95	11.20± 6.88	1.53
10a	7.72±0.78	7.72±0.78	12.35±1.23	5.75 ± 0.45	ND	18.45 ± 4.07	15.17 ± 1.37	1.22
10b	4.72±0.47	4.72±0.47	10.35±1.13	2.85 ± 0.55	1.45± 0.45	8.45 ± 4.07	14.17 ± 1.37	0.59
13	11.23±1.17	12.23±1.47	ND	ND	5.56± 0.55	10.98±1.07	ND	ND
cisplatin	9.66±0.45	5.30±0.45	32.48±1.49	9.60±0.60	13.60±1.30	42.89±1.89	10.20±0.89	4.01
FI[c]	2.05	1.12	3.14	3.37	9.37	5.08	0.72	6.80
Oxaliplatin	11.27±0.85	8.89±0.85	17.72±0.89	11.62±0.78	14.62±0.78	27.61 ± 5.17	10.00±1.23	2.76
FI[d]	2.39	1.88	1.71	4.08	10.08	3.27	0.71	4.70

[a] An average of three measurements. ND = Not determined.
[b] The RF (resistance factor) is defined as the IC_{50} value in A549cisR cells/IC_{50} value in A549 cells.
[c] FI (fold increase) is defined as IC_{50}(cisplatin)/IC_{50}(**10b**).
[d] FI (fold increase) is defined as IC_{50}(oxaliplatin)/IC_{50}(**10b**).

2. RESULTS AND DISCUSSION

2.1 Synthesis and Characterization of Naphthalimides-Pt(IV) Conjugates.

We provided feasible routes to **9a-9b, 10a-10b** in Scheme 1 and the details were given in detail in the supporting information. In this series, compounds **5** and **8** have been reported by our group. [11] The asymmetrically functionalized Pt(IV) compounds **9a-9b, 10a-10b** can be obtained by the reaction of oxide-cisplatin and oxide-oxaliplatin with **5** or **8**. [4] To a solution of oxide-cisplatin or oxide-oxaliplatin (0.38 mmol) in DMF (10 mL) was added a DMF solution (0.5 mL) containing HATU (0.57 mmol). A DMF solution containing **5** or **8** (1.5 mmol) and DIPEA (0.92 mmol) were added to the resulting solution. The mixture was stirred at room temperature for 24 h in the dark. The DMF was then removed under vacuum to afford a yellow oil. Compounds **9a-9b, 10a-10b** was purified by silica gel column chromatography as a yellow solid in a yield of 40%-50%. All new compounds were unambiguously characterized by NMR spectroscopy (^{1}H and ^{13}C), elemental analysis and electrospray ionization (ESI) mass spectrometry. (Figures S1-S12) The purity of Pt complexes was confirmed to be ⩾ 95% by analytical HPLC (Table S1 and S2).

2.2 *In Vitro* Cytotoxicity Effects.

Firstly, the *in vitro* anticancer activity was assessed by the MTT assay in human cancer cell lines including colorectal cancer (HT-29 and HCT-116), lung carcinoma (cisplatin-sensitive A549 and cisplatin-resistant A549cisR) and breast cancer (MDA-MB-231 and MCF-7). (Table 1) Cisplatin and oxaliplatin were chosen as references. The resistance factor (RF) were calculated by the ratio between IC_{50} values calculated for the resistant cells and those obtained with the sensitive cells to evaluate the cross-resistance profiles.

Among mononitro-naphthalimide conjugates (**9a-9b**, **10a-10b**), compound **10b** with the cisplatin core exhibits crucial better cytotoxicity than **9a**, **9b**, **10a** and the positive control cisplatin and oxaliplatin**,** indicating that naphthalimide plays an important role in the Pt(IV) conjugates. Different attached

position in the naphthalimide and different platinum(IV) core significantly affect the bioactivities of target compounds. For compounds **9**–**10**, **10** with cisplatin core exhibits more prominent activities than **9**. And 4-nitro naphthalimide conjugates **9b** and **10b** increase the anticancer efficacy in comparison with 3-nitro **9a** and **10a.** Thus, 4-nitro naphthalimide platinum(IV) complex **10b** was selected for further modification. In addition, the RF of **10b** (RF = 0.59) was 4.70-6.80 folds lower than cisplatin (RF = 4.01) and oxaliplatin (RF = 2.76), indicating its prominent properties to overcome cisplatin resistance. Furthermore, comparing different types of cancer cells, the FI values for **10b** in A549cisR cells were the highest (FI = 5.08), and the FI values in A549 cells were the lowest (FI = 0.72), indicating significant cell selectivity and therapeutic effects to the resistant cells. And also **10b** (FI 1.71-3.14) exerts more prominent activities for triple negative breast cancer (TNBC) MDA-MB-231 than cisplatin and oxaliplatin.

Among these naphthalimide conjugates, **10b** displayed the highest cytotoxicity and significant cell selectivity to the resistant cells. Therefore, more efforts were done to explore the underlying molecular mechanism of **10b** to overcome cisplatin resistance.

2.3 The Stability of 10b in water and RPMI 1640.

Subsequently, the stability of mononitro-naphthalimide conjugate **10b** in water and RPMI 1640 were evaluated. Representative chromatogram was shown in Figure S13. We can observe the enhanced stability that approximately 90% and 80% of **10b** remained unchanged even after 72 h in water and RPMI-1640, respectively. (Figure 2)

a. b.

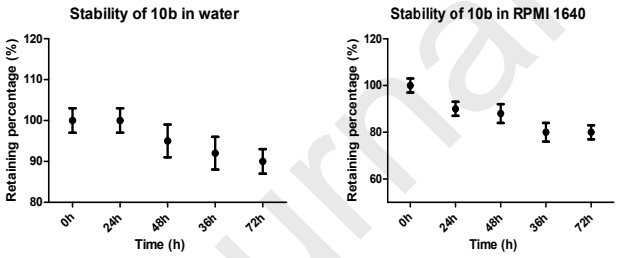

Figure 2. Stability of compound **10b** in water and RPMI-1640 tested by RP-HPLC at room temperature in dark. a) Stability of compound **10b** in water. b) Stability of compound **10b** in RPMI-1640.

2.4 *In Vitro* Cell Selectivity of 10b to Cancer Cells and the Matched Normal Cells.

Table 2. IC_{50} values (μM) of Pt(IV) prodrugs. Cells were treated for 48 h, and the cell viability was determined by MTT assays[b]

	SMMC7721	HL-7702	SI [a]
10b	10.92±0.69	28.48±1.45	2.61
Cisplatin	23.37±1.26	5.6±0.20	0.24
Oxaliplatin	11.77±1.88	6.77±0.78	0.58

[a] SI(selectivity index) is defined as IC_{50} in HL-7702/IC_{50} in SMMC7721.

[b] An average of three measurements.

As shown in Table 2, *in vitro* cell selectivity of **10b** to cancer cells and the matched normal cells were further determined. We can see that the selectivity index (SI) values of **10b** (SI = 2.61) were 5-11 folds higher than that of cisplatin (SI = 0.24), oxaliplatin (SI = 0.58), indicating a lower toxicity to normal cells than the matched cancer cells. We also measured the cellular drug uptake in cancer cells and matched normal cells by ICP-MS. The cell drug uptake of **10b** in SMMC-7721 was 2.5 times higher than that of HL-7702 (Figure 3), which is in accordance with the results of MTT assay.

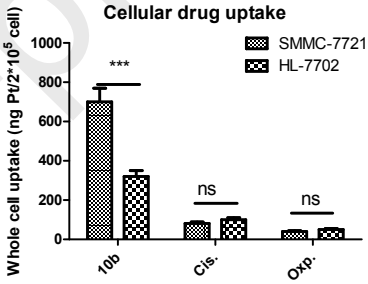

Figure 3. Cellular uptake and distribution of **10b** in cancer cells and matched normal cells with 10 μM of tested complexes.

2.5 *In Vivo* Maximum Tolerated Dose (MTD) and the Lethal Dose (LD_{50}) Values.

Table 3. *In vivo* maximum tolerated dose and lethal dose values and calculated therapeutic indices (LD_{50}/IC_{50}) of **10b**, cisplatin and oxaliplatin. The maximum tolerated dose (MTD) was evaluated by calculating body weight loss (mean weight loss < 15% and < 15% toxic deaths).

Complexes	MTD (mg/kg)	LD_{50} (mg/kg)	LD_{50} (μM/kg)	48 h Avg IC_{50} (μM)	LD_{50}/IC_{50}
10b	30.00	60.00	65.00	3.85	16.88
cisplatin	9.00	16.00	53.69	9.60	5.59

Oxaliplatin	15.00	30.00	75.56	11.62	6.50

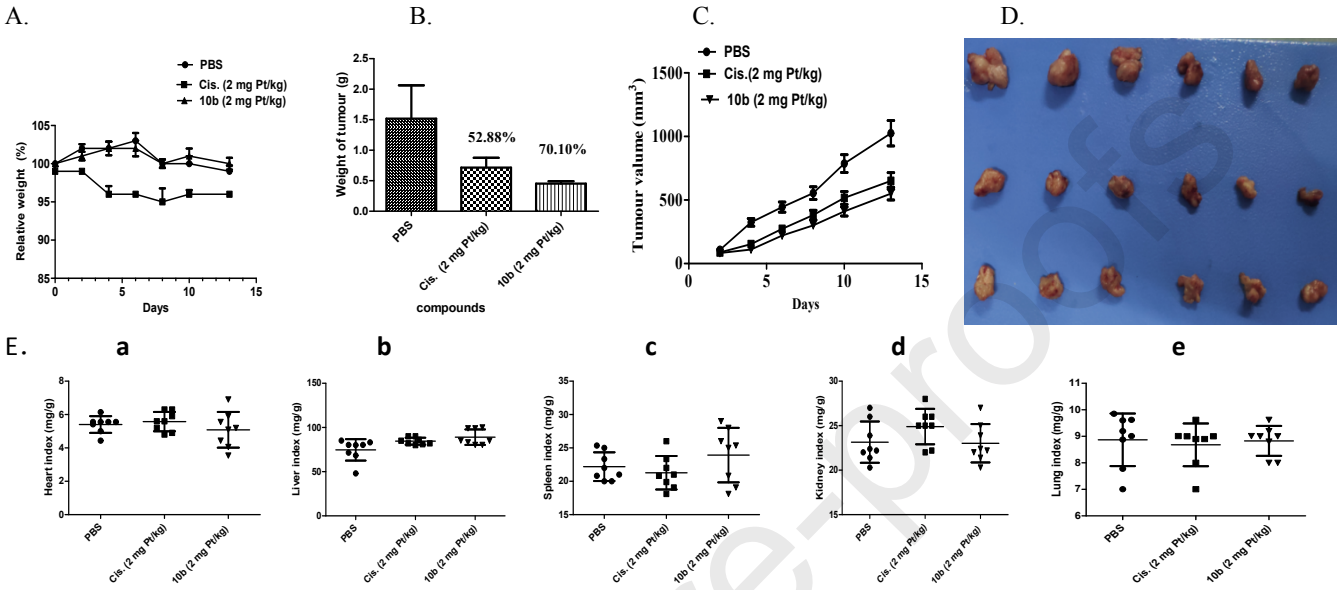

Figure 4. *In vivo* antitumour activities of compounds **10b** and cisplatin in 4T1 breast carcinoma tumours. (A) The body weight of the mice during the treatment. (B) The tumour weight in each group at the end of the experiment. (C) Tumour growth as a function of time. (D) Images of the tumours at the end of the experiment. (E) Organ weight indexes (a. heart, b. liver, c. spleen, d. lung, and e. kidney) after treatment with **10b**, cisplatin, and normal saline *in vivo*. The first line, the control group; the second line, cisplatin, 2 mg Pt/kg; the third line, **10b**, 2 mg Pt/kg.

Our laboratories [11] and others [9, 12] previously emphasized the pivotal evidences that some naphthalimide conjugates could potently inhibit tumour growth and metastasis by multiple pathways including DNA dysfunction *in vitro* and *in vivo*. Next, we conducted an acute toxicity study using BALB/c mice to evaluate the potential safety of the naphthalimide conjugates. The maximum tolerated dose (MTD) and the lethal dose (LD_{50}) values were determined as summarized in Table 3.

Both the MTD and LD_{50} values of **10b** were 3-4 folds higher than those of cisplatin and oxaliplatin, indicating that **10b** may have significantly enhanced the feasibility and potential safety of high-dose treatment. The ratios of the cytotoxicity (IC_{50}) towards MCF-7 cells to LD_{50} of **10b** were used as a measure of the therapeutic index (TI). The results showed that **10b** (TI = 16.88) were the safest complex than that of cisplatin (TI =5.59) and oxaliplatin (TI = 6.50), indicating that it may potentially allow an adequate margin of safety *in vivo* and clinical therapeutic exposure.

Next, we further investigated the *in vivo* antitumour activities of **10b** in 4T1 breast carcinoma tumours and the results are shown in Figure 4. At the same dose, the di-functionalized Pt(IV) derivative **10b** remarkably suppresses tumour growth with a 70.10% inhibition rate, which is comparable to cisplatin (52.88%). (Figure 4B) However, upon cisplatin treatment, the weight of the mice decreased significantly to 95% of the initial weight, whereas the weight loss in the **10b**-treated groups was 102%-100%, indicating significant inhibition effects and lower toxicity *in vivo* (Figure 4A). Moreover, on day 13, the average tumour volume was 550 mm^3 upon **10b** treatment, and this value was 1025 mm^3 for the control group. (Figure 4C) Organ weight indexes of heart, liver, spleen, lung, and kidney after treatment with **10b**, cisplatin, and normal saline were also tested as shown in Figure 4E. For the first time, we found the significant antitumor activities of the Pt(IV) derivative **10b** *in vitro* and *in vivo*, which shows highly efficient tumour inhibition and lower toxicity *in vitro* and *in vivo*. Next, we made more efforts to explore the molecular mechanism.

2.6 *In Vivo* Antitumor Activities.

2.7 ICP-MS Determination of Cellular Accumulation and Binding to Nuclear DNA.

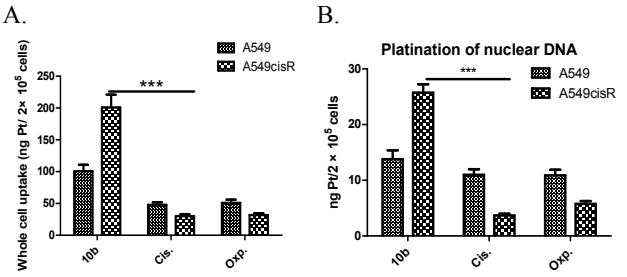

Figure 5. Cellular uptake and distribution of 10 μM **10b** and cisplatin and oxaliplatin following 8 h incubation in A549 and A549cisR cells. (A) Pt accumulation in A549 and A549cisR cells upon 10 μM treatment for 8 h. (B) Platination levels of nuclear DNA extracts of A549 and A549cisR cells after 8 h incubation with 10 μM tested compounds. ***, P< 0.001.

In order further to determine mononitro-naphthalimide Pt(IV) complex to the DNA damage, the ability of **10b** binding with nucleotides in A549 and A549cisR cells were further determined. The results were summarized in Figure 5 as ng Pt per 2×10^5 cells. The Pt accumulation (200.91 ng/2×10^5 cells) and the genomic DNA Pt levels (25.74 ng/2×10^5 cells) after treated with 10 μM **10b** are much higher than that of cisplatin with 30.14 ng/2×10^5 cells and 3.69 ng/2×10^5 cells, respectively. The results above indicates that **10b** exhibited preferentially enhanced DNA damage. In addition, the cellular accumulation and genomic DNA Pt levels from **10b** in A549cisR cells are 2 folds higher than those in A549 cells, which is in accordance with the results in Table 1. We can deduce that **10b** elicited impressive cytotoxic activity and cell selectivity to A549cisR cells probably by enhanced DNA damage.

2.8 The Ability of 10b to Induce Apoptosis and Increase the Expression Level of Phospho-histone H2A.X, p53 and RAD51 in A549cisR Cells.

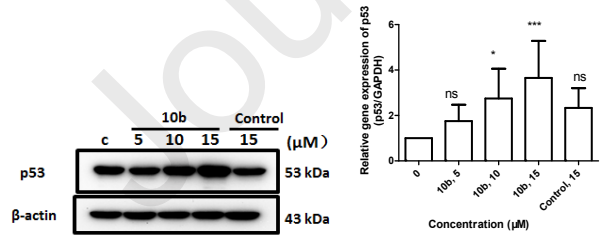

Figure 6. Effects of different concentrations of **10b** and cisplatin on p53 transcript level by qRT-PCR analysis (A) and the p53 protein level (B) in A549cisR cells. *, P< 0.05; ***, P< 0.001.

To further determine whether **10b** are able to cause DNA damage within a certain time, the ability of **10b** to induce apoptosis and increase the expression level of the p53 transcript level by qRT-PCR analysis and the p53 protein level in A549cisR cells were determined by Western blotting, which also played an important role in cell apoptosis and cisplatin resistance. Compared with cisplatin and the control group, **10b** remarkably upregulated the p53 gene and p53 protein in A549cisR cells (Figure 6). H2A.X plays a key role in DNA repair, and phosphorylation of Ser139 will occur to form γH2A.X rapidly after the formation of DNA doublestrand breaks (DSBs) to block the DNA damage repair.[13] Therefore, γH2A.X transcript and protein level were further determined in Figure 7. Compared to cisplatin, **10b** evokes a remarkably higher level of γH2A.X than cisplatin and oxaliplatin in A549cisR cells after 24 h.

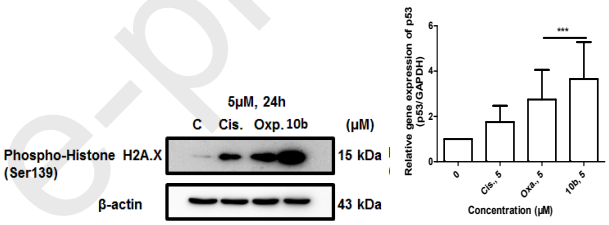

Figure 7. Effects of different concentrations of **10b** and cisplatin on γH2A.X transcript and protein level in A549cisR cells. (A) Effect of **10b** and cisplatin on γH2A.X expression in A549cisR cells after 24 h of treatment. (B) qRT-PCR analysis of the γH2A.X transcript level was performed with total RNAs purified from A549cisR cells treated with **10b** and cisplatin for the indicated times. *, P< 0.05; ***, P< 0.001.

Next, we examined the expression of RAD51 in A549cisR cells to further ascertain whether DNA repair is involved in the process of DNA damage. [14] RAD51 is also a key factor for initiating the homologous recombination of DNA after double-strand breaks and essential for the repair of replication-stalling lesions caused by DNA-damaging agents. [15] The up-regulation of RAD51 suggested that the DNA damage repair was inhibited. Instead, it was the repair that was inhibited. Remarkably, compared with the cisplatin-treated groups, the expression of RAD51 gene and protein was evidently decreased by **10b** (Figure 8). These results imply that in comparison to that of cisplatin**, 10b** not only induced severe DNA damage, but also inhibited the repair of DNA damage, thus resulting in its higher cytotoxicity. Currently, it is still indistinct for the reason of the inhibition of RAD51 by **10b** .

A. B.

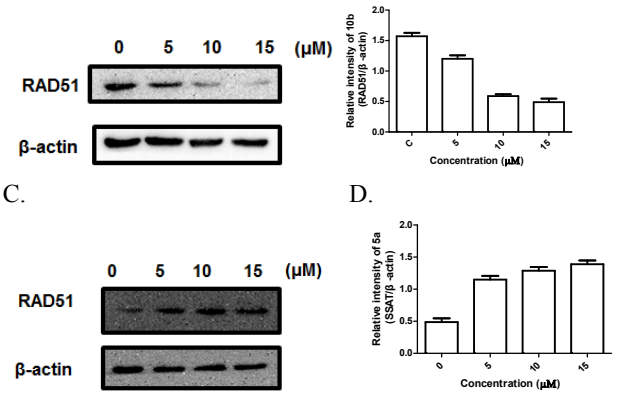

Figure 8. Effect of **10b** (A) or cisplatin (C) on RAD51 expression in A549cisR cells after 24 h of treatment. qRT-PCR analysis of the RAD51 transcript level was performed with total RNAs purified from A549cisR cells treated with **10b** (B) and cisplatin (D) for the indicated times.

2.10 Reduction and DNA binding properties of 10b and cisplatin with and without ascorbic acid.

Subsequently, in order to further determine the binding properties of **10b** with DNA, we measured the reduction and DNA-binding properties of **10b** with ascorbic acid. (Figure 9) Using 5'-dGMP as a DNA model, the DNA-binding properties of **10b** (1 mM) with 5'-dGMP (3 mM) in the presence of ascorbic acid (5 mM) were determined by RP-HPLC after incubation 37 ℃ for 24 h and 48 h. The unknown peak fractions as adducts (Figure 9a) were separated and identified as cis-Pt(II)-GMP by ESI-MS analysis. Meanwhile, the same product was observed after treatment of cisplatin. The possible mechanism of **10b** reacted with 5'-dGMP in the presence of ascorbic acid was also shown in Figure 9b. We deduced that **10b** was generated by the combination of cisplatin with 5'-dGMP after reduction by ascorbic acid.

a.

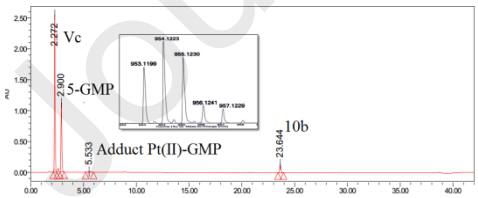

b.

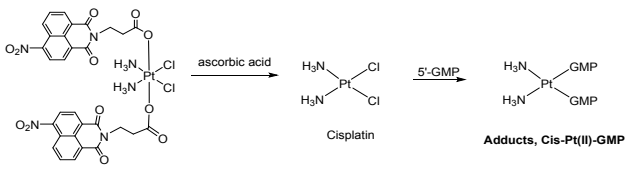

Figure 9. Compound **10b** binding with 5'-dGMP as DNA model. a) Reduction and DNA-binding properties of 10b with ascorbic acid after 24 h, and 48 h. b) The possible mechanism of compound **10b** reaction with 5'-dGMP in the presence of ascorbic acid incubated at 37 °C after 24 h.

3. CONCLUSIONS.

Taken together, our findings provided the first example of mononitro-naphthalimide Pt(IV) drug **10b** targeting DNA damage repair via dual DNA damage mechanism by promoting RAD51 pathway to overcome cisplatin resistance. Comparing different types of cancer cells, the FI values for **10b** in A549cisR cells were the highest (FI = 5.08), and the FI values in A549 cells were the lowest (FI = 0.72), indicating significant cell selectivity and therapeutic effects to the resistant cells. *In vitro* cell selectivity of **10b** to cancer cells and the matched normal cells indicates a lower toxicity to normal cells than the matched cancer cells. Both the MTD and LD_{50} values indicate that **10b** may have significantly enhanced the feasibility and potential safety of high-dose treatment. **10b** remarkably suppresses tumour growth with a 70.01% inhibition rate, which is comparable to cisplatin (52.88%). The Pt accumulation (200.91 ng/2×10^5 cells) and the genomic DNA Pt levels (25.74 ng/2×10^5 cells) after treated with 10 μM **10b** are much higher than that of cisplatin by upregulating p53/γH2A.X/RAD51. The discovery of the potential role of naphthalimide-Pt(IV) prodrugs broadens our strategy for the design of more potential anticancer agents through multiple pathways involving DNA dysfunction, prolongs the life of cancer and overcomes cisplatin resistance in a totally new field.

4. EXPERIMENTAL SECTION.

4.1 General Procedure for the Synthesis of Compound 9a.

A DMF solution (0.5 mL) containing HATU (0.57 mmol) was added to a solution of **5** (0.38 mmol) in DMF (10 mL). The mixture was stirred at room temperature for 10 minutes. A DMF solution containing DIPEA (0.92 mmol) and oxide-oxaliplatin (1.5 mmol) was added to the resulting solution. The mixture was stirred at room temperature for 24 hours in the dark. The DMF was then removed under vacuum to give a yellow oil. Compound **9a** was purified as a yellow solid by silica gel column chromatography with a yield of 47%. ^{1}H NMR (300 MHz, Methanol-d_4) δ 7.89 – 7.82 (m, 2H), 7.80 – 7.72 (m, 2H), 7.53 (qd, J = 7.2, 1.2 Hz, 4H), 3.19 (d, J = 7.3 Hz, 4H), 1.35 (s, 8H). ^{13}C NMR (75 MHz, DMSO-d_6) δ 178.48 , 172.33 , 171.13 , 170.51 , 164.27 , 163.16 , 163.08 , 162.67 , 162.56 , 146.11 , 143.11 , 136.78 , 136.70 , 134.36 , 131.17 , 130.10 , 129.84 , 129.66 , 128.20 , 127.77 , 126.63 , 125.11 , 124.31 , 124.11 , 123.21 , 122.86 , 119.41 , 119.03 , 111.41 , 110.10 , 61.26 , 51.87 , 46.26 , 42.50 , 37.02 , 35.58 , 35.09 , 34.00 , 9.04 . ESI-MS (positive ion mode): m/z [M]$^+$:

calcd: 1023.1523; obsd: 1023.1552. Calcd for $C_{38}H_{32}N_6O_{16}Pt$: C 44.58%, H 3.15%, N 8.21%. Found: C 44.26%, H 3.02%, N 8.03%.

4.2 General Procedure for the Synthesis of Compound 9b.

A DMF solution (0.5 mL) containing HATU (0.57 mmol) was added to a solution of **8** (0.38 mmol) in DMF (10 mL). The mixture was stirred at room temperature for 10 minutes. A DMF solution containing DIPEA (0.92 mmol) and oxide-oxaliplatin (1.5 mmol) was added to the resulting solution. The mixture was stirred at room temperature for 24 hours in the dark. The DMF was then removed under vacuum to give a yellow oil. Compound **9b** was purified as a yellow solid by silica gel column chromatography with a yield of 37%.

^{1}H NMR (300 MHz, Chloroform-*d*) δ 8.40 (dd, *J* = 8.0, 2.5 Hz, 1H), 7.93 – 7.78 (m, 2H), 7.79 – 7.69 (m, 3H), 7.51 (dddd, *J* = 18.5, 8.1, 6.9, 1.2 Hz, 4H), 3.22 (q, *J* = 7.3 Hz, 8H), 1.31 (t, *J* = 7.3 Hz, 13H).^{13}C NMR (75 MHz, Chloroform-*d*) δ 175.66 , 175.29,174.69 , 168.46,168.22,168.17 , 150.75 , 137.65 , 135.85 , 135.78 , 134.94 , 130.59 , 130.44 , 126.60 , 126.01 , 125.76 , 125.72 , 117.77 , 117.72 , 69.33 , 46.14 , 44.04 , 40.68 , 40.25 , 38.39 , 35.10 , 33.37 , 23.10 , 17.22 , 15.96 , 13.58 . ESI-MS (positive ion mode): m/z [M]+: calcd: 1023.1523; obsd: 1023.1507. Calcd for $C_{38}H_{32}N_6O_{16}Pt$: C 44.58%, H 3.15%, N 8.21%. Found: C 44.21%, H 3.05%, N 8.02%.

4.3 General Procedure for the Synthesis of Compound 10a.

A DMF solution (0.5 mL) containing HATU (0.57 mmol) was added to a solution of **5** (0.38 mmol) in DMF (10 mL). The mixture was stirred at room temperature for 10 minutes. A DMF solution containing DIPEA (0.92 mmol) and oxide-cisplatin (1.5 mmol) was added to the resulting solution. The mixture was stirred at room temperature for 24 hours in the dark. The DMF was then removed under vacuum to give a yellow oil. Compound **10a** was purified as a yellow solid by silica gel column chromatography with a yield of 40%. ^{1}H NMR (300 MHz, DMSO-d_6) δ 9.32 (d, *J* = 9.6 Hz, 1H), 8.82 (d, *J* = 2.4 Hz, 1H), 8.63 (dd, *J* = 22.8, 7.7 Hz, 2H), 8.03 – 7.91 (m, 2H), 7.68 (d, *J* = 8.3 Hz, 1H), 7.53 (t, *J* = 7.6 Hz, 1H), 7.40 (t, *J* = 7.7 Hz, 1H), 3.08 (q, *J* = 7.3 Hz, 5H), 2.53 (d, *J* = 12.0 Hz, 6H), 1.17 (t, *J* = 7.2 Hz, 8H). ^{13}C NMR (75 MHz, DMSO-d_6) δ 179.25 , 178.47 , 173.46 , 170.50 , 163.01 , 162.48 , 146.03 (d, *J* = 4.4 Hz), 143.10 , 136.68 , 135.17 – 133.89 (m), 131.08 (d, *J* = 5.2 Hz), 130.17 – 129.48 (m), 127.84 (d, *J* = 49.2 Hz), 124.99 , 124.22 , 122.97 (d, *J* = 24.5 Hz), 119.34 , 110.17 , 46.25 , 37.28 , 35.16 , 33.87 , 9.04 . ESI-MS (positive ion mode): m/z $[M]^+$: calcd: 925.0577; obsd: 925.0546. Calcd for $C_{30}H_{24}Cl_2N_6O_{12}Pt$: C 38.89%, H 2.61%, N 9.07%. Found: C 38.72%, H 2.42%, N 8.92%.

4.4 General Procedure for the Synthesis of Compound 10b.

A DMF solution (0.5 mL) containing HATU (0.57 mmol) was added to a solution of **8** (0.38 mmol) in DMF (10 mL). The mixture was stirred at room temperature for 10 minutes. A DMF solution containing DIPEA (0.92 mmol) and oxide-cisplatin (1.5 mmol) was added to the resulting solution. The mixture was stirred at room temperature for 24 hours in the dark. The DMF was then removed under vacuum to give a yellow oil. Compound **10b** was purified as a yellow solid by silica gel column chromatography with a yield of 40%. ^{1}H NMR (300 MHz, Chloroform-*d*) δ 9.25 – 8.38 (m, 1H), 7.91 – 7.64 (m, 1H), 7.46 – 7.28 (m, 1H), 3.21 (q, *J* = 7.2 Hz, 8H), 1.35 (t, *J* = 7.2 Hz, 6H). ^{13}C NMR (75 MHz, DMSO-d_6) δ 181.37 , 180.92 , 172.85 , 171.97 , 163.49 , 162.50 , 149.58 , 143.25 (d, *J* = 1.9 Hz), 130.56 , 130.10 , 129.20 , 128.95 , 128.80 , 128.27 , 127.82 , 127.20 , 126.42 , 124.98 , 124.71 , 123.88 , 123.32 , 123.21 , 119.59 , 119.08 , 111.47 , 110.06 , 46.17 , 31.76 , 29.54 , 22.57 , 14.42 , 9.08 . ESI-MS (positive ion mode): m/z $[M+K]^+$: calcd: 965.3343; obsd: 965.3355. Calcd for $C_{30}H_{24}Cl_2N_6O_{12}Pt$: C 38.89%, H 2.61%, N 9.07%. Found: C 38.72%, H 2.51%, N 8.98 %.

4.5 *In Vitro* Cellular Cytotoxicity Assays.

In a 5% CO_2 atmosphere, cells (5000/well) were incubated in 100 μL RPMI or DMEM medium in a 96-well plate at 37 ° C for 24 hours. Then, in freshly prepared medium (100 μL), we dissolved the drug in different concentrations, and incubated for 48 hours after adding the drug. Prepare MTT at 5 mg / mL, add 20 μL, and incubate for another 3 hours. Finally, remove the medium and add 150 μL of DMSO to dissolve the purple crystals. The absorbance was measured at 570 nm by a Bio-Rad 680 microplate reader. IC_{50} values were counted based on three parallel experiments using GraphPad Prism software.

4.6 *In vivo* Antitumor Assays.

5-week-old female BALB / c mice (Cat. SCXK 2016-0006) (weight 18-22 g) were purchased from the Experimental Animal Center of Beijing Academy of Military Medical Sciences. According to the "Guidelines for Laboratory Animal Care" issued by Henan University, all animal experiments have been approved by the Ethics Committee (HUSOM-2016-316).

In vivo antitumour activity, 4T1 cells (1×10^6 cells per mouse) were injected subcutaneously in mice and allowed to proliferate for 7 days. When the tumor grows to 80 – 120 mm^3, the drug **10b** (2.0 mg Pt/kg), cisplatin (2.0 mg Pt/kg, positive control) or saline (dissolved in glucose solution *via* tail vein injection every two days (negative control), do four treatments Group of eight mice. Body weight and tumour volume were measured once every two days. After the experiment, the mice were sacrificed and the tumour tissue was weighed at the same time. The inhibition rate was calculated as follows: inhibition rate (%) = [(average tumour weight of control group - the average tumour weight of the drug-treated or positive group) / the average tumour weight of the control group] × 100).

4.7 *In vivo* MTD and LD_{50} Antitumor Assays.

The MTD was calculated by mean weight loss <15% and poisoning death <15%. LD_{50} and TI values are calculated based on previous reports. [6b]

4.8 ICP-MS Determination of Cellular Accumulation and Binding to Nuclear DNA.

Using A549 and A549cisR cells, cells (2×10^5 cells / well) were seeded into 6-well plates and incubated for 24 hours. After adding 10 μM **10b**, cisplatin or oxaliplatin for 8 hours, we washed the cells 3 times with PBS and then collected the cells by trypsin digestion. Count the number of cells before digestion, then concentrate the harvested cells, we digest with nitric acid and evaporate for ICP-MS. To isolate DNA, Genomic DNA mini preparation kit was used. After the DNA was collected, it was performed by ICP-MS according to the similar method described above in A549 and A549cisR.

4.9 Annexin V-FITC/Propidium Iodide Staining.

Through annexin V-FITC/PI staining and flow cytometry (BD Biosciences, San Jose, California, USA), we evaluated the apoptosis of A549cisR cells. After incubating cells (1×10^5 cells / well) in a six-well plate for 24 hours, add **10b** (5 or 10 μM) or cisplatin (15 μM) and incubate for another 24 h. The cells were then washed 3 times with PBS, collected and stained by flow cytometry according to standard protocols.

4.10 Western Blot Assay.

Phospho-histone H2A-X (Ser139), p53 and RAD51 detected by Western blot analysis. A549cisR cells were seeded in 6 well plates, and incubated for 24 hours. 5, 10 and then added to 15 μM **10b** and then incubated for 24 hours. Then cells were harvested, washed with PBS 3 times by centrifugation and lysed. Total protein was measured by BCA assay kit (Beyotime, China). Denature the total lysate in 5 × SDS loading buffer at 100 ° C for 10 minutes. The total protein was separated by 12% SDS-PAGE for another 2 hours and transferred to PVDF membrane. Then placed in TBST at room temperature for 1 h, we blocked the PVDF membrane with 5% skim milk and incubated with the corresponding antibody and HRP-conjugated secondary antibody. The protein content was detected using ECL plus reagents (Beyotime, Jiangsu Province, China).

4.11 Methods for stability of 10b in water and RPMI 1640 and purity determination of 9a-9b, 10a-10b.

Table 3. Method for stability of **9a-9b, 10a-10b** in water and RPMI 1640 and purity determination of **9a-9b, 10a-10b** by analytical HPLC. Injection volume was 20 μL (0.5mL/min). The absorbance wavelength of HPLC was set to 254 nm and 365 nm, and the percentages of Pt(IV) compounds remaining were calculated by the ratio of peak areas at 254 nm.

Time (min)	A (water)	B (methanol)
	95%	5%
20	95%	5%
30	50%	50%

We determined the stability of **10b** in water and RPMI 1640 and the purity of **9a-9b**, **10a-10b**, and **10b** in HPLC (Waters E2695-2998 equipped with a Venusil MP C18 column (150 × 4.6 mm, 5 μm)) The stability of RPMI 1640 in water is shown in Figure 3. Under the same conditions, we confirmed that the purity of **9a-9b** and **10a-10b** was ≥95% by analytical HPLC, and had the same stability in water and RPMI 1640. Table 3 shows the purity measurement results of **9a-9b** and **10a-10b**, and Table 4 shows the purity measurement results of **9a-9b** and **10a-10b**.

4.12 Method for reaction of oxaliplatin and 10b with 5'-dGMP in the presence and absence of ascorbic acid.

HPLC analysis was also performed on Waters E2695-2998 equipped with a Venusil MP C18 column (150 × 4.6 mm, 5 μm). [7b-7e] Using RP-HPLC to determine the absence of ascorbic acid at 37 ° C, the DNA binding characteristics of cisplatin (1 mM) and 5'-dGMP (1 mM) were determined using 5'-dGMP as the DNA model. We also determined the presence of **10b** (1 mM) and 5'-dGMP (3 mM) in the presence of ascorbic acid (5 mM) at 0 hours, 24 hours, 48 hours, 72 hours and 96 hours (5 mM) reaction. The injection volume was 20 μL (0.5 mL/min). The absorbance wavelength of HPLC was set to 254 nm and 365 nm, and the percentage of the remaining Pt (IV) compound was calculated by the ratio of the peak areas at 254 nm. The HPLC procedure is as follows: 95% (water) to 5% (methanol) for 20 minutes; m/z ($M+H^+$). 50% (water) to 50% (methanol) (linear increase from 21 minutes to 30 minutes). The results prove that ascorbic acid can reduce the platinum (IV) complex and release the Pt (II) complex. Then, the Pt (II) compound was combined with 5'-dGMP to form cis-Pt (II) -GMP, and confirmed by HRMS.

ASSOCIATED CONTENT

The Supporting Information is available free of charge on the ACS Publications website.
Full experimental details, NMR data, and bioassay information (PDF)

AUTHOR INFORMATION

Corresponding Author *Phone: (86) 0371-23880680. Fax: (86) 0371-23880680.E-mail: wangjiajia1359334@163.com; majing@henu.edu.cn; xiesq@vip.henu.edu.cn

Abbreviations

PTs, Polyamine Transporters; SSAT, spermidine/spermine N1-acetyltransferase; PAO, N1-acetylpolyamine oxidase; ROS, Reactive Oxygen Species; GSH-Px, glutathione peroxidase; GSH, glutathione; Spd, spermidine; Spm, spermine; Put, putrescine. LD_{50}, lethal dose of 50%; MTD, maximum tolerated dose; IC_{50}, half maximal inhibitory concentration; ICP-MS, Inductively Coupled Plasma Mass Spectrometry; DMF, dimethyl formamide; DIPEA, diisopropylethylamine; HATU, 2-(7-Azabenzotriazol-1-yl)-N,N,N',N'-tetramethyluronium hexafluorophosphate.

Notes

The authors declare no competing financial interest.

ACKNOWLEDGMENTS

This work was supported by National Natural Science Foundation of China (Grant No. 21807025, 81772832 and 21907022), China Postdoctoral Science Foundation (Grant No. 2018M640673), Postdoctoral Research Grant in Henan Province (Grant No. 001802020), Key Scientific Research Projects in Henan Colleges and Universities (Grant No. 19A350002), Program for Innovative Research Team (in Science and Technology in University of Henan Province) (Grant No. 19IRTSTHN004), Scientific Research Cultivating Program for Young Talents in Henan Medical School (Grant No. 2019006) and the key scientific research projects of universities in Henan province (202102310471).

REFERENCES

[1] a) D. Wang, S. J. Lippard, Cellular processing of platinum anticancer drugs. **Nat. Rev. Drug Discovery** 2005, 4, 307 – 320; b) Zhiqin D , Na W , Yingying L, Zoufeng X, Zhigang W, Tai-Chu L , Guangyu Z. A Photocaged, Water-Oxidizing, and Nucleolus-Targeted Pt(IV) Complex With a Distinct Anticancer Mechanism. **J Am Chem Soc.** 2020, 142, 7803-7812; c) L. Kelland, The resurgence of platinum-based cancer chemotherapy. **Nat. Rev. Cancer** 2007, 7, 573 – 584; d) T. Boulikas, M. Vougiouka, Recent clinical trials using cisplatin, carboplatin and their combination chemotherapy drugs (review). **Oncol. Rep.** 2004, 11, 559 – 595; e) B. A. Chabner, T. G. Roberts, Jr., Timeline: Chemotherapy and the war on cancer. **Nat. Rev. Cancer** 2005, 5, 65 –72; f) Imran, M.; Ayub, W.; Butler, I. S.; Zia-ur-Rehman. Photoactivated platinum-based anticancer drugs. **Coord. Chem. Rev.** 2018, 376, 405−429.

[2] a) R. P. Miller, R. K. Tadagavadi, G. Ramesh, W. B. Reeves, Mechanisms of Cisplatin nephrotoxicity. **Toxins** 2010, 2, 2490 – 2518. b) Oun, R.; Moussa, Y. E.; Wheate, N. J. The side effects of platinum-based chemotherapy drugs: a review for chemists. **Dalton Trans.** 2018, 47, 6645−6653.

[3] a) C. J. Lord, A. Ashworth, The DNA damage response and cancer therapy. **Nature** 2012, 481, 287–294; b) P. Bouwman, J. Jonkers, The effects of deregulated DNA damage signalling on cancer chemotherapy response and resistance. **Nat. Rev. Cancer** 2012, 12, 587– 598; c) P. A. Jeggo, L. H. Pearl, A. M. Carr, DNA repair, genome stability and cancer: a historical perspective. **Nat. Rev. Cancer** 2016, 16, 35– 42.

[4] a) L. H. Pearl, A. C. Schierz, S. E. Ward, B. Al-Lazikani, F. M. Pearl, Therapeutic opportunities within the DNA damage response. **Nat. Rev. Cancer** 2015, 15, 166– 180. b) S. P. Jackson, J. Bartek, The DNA-damage response in human biology and disease. **Nature** 2009, 461, 1071–1078. c) Wang Z, Xu Z, Zhu G. A Platinum(IV) Anticancer Prodrug Targeting Nucleotide Excision Repair To Overcome Cisplatin Resistance. **Angew Chem Int Ed Engl.** 2016, 55, 15564-15568.

[5] a) D. Gibson, Platinum(iv) anticancer prodrugs - hypotheses and facts. **Dalton Trans.** 2016, 45, 12983 – 12991; b) T. C. Johnstone, K. Suntharalingam, S. J. Lippard, The Next Generation of Platinum Drugs: Targeted Pt(II) Agents, Nanoparticle Delivery, and Pt(IV) Prodrugs. **Chem. Rev.** 2016, 116, 3436 – 3486. c) Basu U, Banik B, Wen R, Pathak RK, Dhar S. The Platin-X series: activation, targeting, and delivery. **Dalton Trans.** 2016, 45, 12992-3004; d) X. Wang, Z. Guo, Targeting and delivery of platinum-based anticancer drugs. **Chem. Soc. Rev.** 2013, 42, 202 – 224. e) Kenny RG, Marmion CJ. Toward Multi-Targeted Platinum and Ruthenium Drugs-A New Paradigm in Cancer Drug Treatment Regimens? **Chem Rev.** 2019, 119, 1058-1137; f) Wang, X.; Wang, X.; Guo, Z. Functionalization of Platinum Complexes for Biomedical Applications. **Acc Chem Res.** 2015, 48, 2622-2631.

[6] Abu Ammar, A.; Raveendran, R.; Gibson, D.; Nassar, T.; Benita, S. A lipophilic Pt(IV) oxaliplatin derivative enhances antitumor activity. **J. Med. Chem.** 2016, 59, 9035−9046.

[7] a) Chen, Y.; Heeg, M. J.; Braunschweiger, P. G.; Xie, W.; Wang, P. G. A Carbohydrate-Linked Cisplatin Analogue Having Antitumor Activity. **Angew. Chem., Int. Ed.** 1999, 38: 1768. b) Ma, J.; Wang, Q.; Huang, Z.; Yang, X.; Nie, Q.; Hao, W.; Wang, P.G.; Wang, X. Glycosylated Platinum(IV) Complexes as Substrates for Glucose Transporters (GLUTs) and Organic Cation Transporters (OCTs) Exhibited Cancer Targeting and Human Serum Albumin Binding Properties for Drug Delivery. **J Med Chem.** 2017, 60: 5736-5748. c) Ma, J.; Wang, Q.; Yang, X.; Hao, W.; Huang, Z.; Zhang, J.; Wang, X.; Wang, P. Glycosylated platinum(iv) prodrugs demonstrated significant therapeutic efficacy in cancer cells and minimized

side-effects. **Dalton Trans.** 2016, 45: 11830−11838. d) Ma, J.; Yang, X.; Hao, W.; Huang, Z.; Wang, X.; Wang, P.G. Mono-functionalized glycosylated platinum(IV) complexes possessed both pH and redox dual-responsive properties: Exhibited enhanced safety and preferentially accumulated in cancer cells in vitro and in vivo. **Eur J Med Chem.** 2017, 128: 45-55. e). Wang, Q.; Huang, Z.; Ma, J.; Lu, X.; Zhang, L.; Wang, X.; Wang, P. G. Design, synthesis and biological evaluation of a novel series of glycosylated platinum(iv) complexes as antitumor agents. **Dalton Trans.** 2016, 45: 10366−10374. f). Ma J, Liu H, Xi Z, Hou J, Li Y, Niu J, Liu T, Bi S, Wang X, Wang C, Wang J, Xie S, Wang PG. Protected and De-protected Platinum(IV) Glycoconjugates With GLUT1 and OCT2-Mediated Selective Cancer Targeting: Demonstrated Enhanced Transporter-Mediated Cytotoxic Properties in vitro and in vivo. **Front Chem.** 2018, 6, 386. g). Ma J, Liu H, Li Y, Yue K, Li L, Xi Z, Zhang X, Liu J, Feng K, Ma Q, Liu S, Guo S, Wang P, Wang C, and Xie S. Polyamine-based Pt(IV) Prodrugs as Substrates for Polyamine Transporters Preferentially Accumulates in Cancer Metastases as DNA and Polyamine Metabolism Dual-Targeted Antimetastatic Agents. **J Med Chem.** 2019, 62, 11324-11334. h). Ma J, Li L, Yue K, Li Y, Liu H, Wang P, Wang C, Wang J, Luo W, Xie S. Bromocoumarinplatin, Targeting Simultaneous Mitochondrion and Cell Nucleus with p53 Apoptosis Pathway to Overcome Cisplatin Resistance. **Bioorganic chemistry**, 2020, doi.org/10.1016/j.bioorg.2020.103768.

[8] a). Dhar S, Daniel WL, Giljohann DA, Mirkin CA, Lippard SJ. Polyvalent oligonucleotide gold nanoparticle conjugates as delivery vehicles for platinum(IV) warheads. **J Am Chem Soc.** *2009*, 131, 14652-14653. b). Liu P, Lu Y, Gao X, Liu R, Zhang-Negrerie D, Shi Y, Wang Y, Wang S, Gao Q. Highly water-soluble platinum(II) complexes as GLUT substrates for targeted therapy: improved anticancer efficacy and transporter-mediated cytotoxic properties. **Chem Commun.** *2013*, 49, 2421-2423. c). Y.-R. Zheng, K. Suntharalingam, T. C. Johnstone, H. Yoo, W. Lin, J. G. Brooks, S. J. Lippard, Pt(IV) prodrugs designed to bind non-covalently to human serum albumin for drug delivery. **J. Am. Chem. Soc.** *2014*, 136, 8790-8798; d). Q. Cheng, H. Shi, H. Wang, Y. Min, J. Wang, Y. Liu, The ligation of aspirin to cisplatin demonstrates significant synergistic effects on tumor cells. **Chem. Commun.** *2014*, 50, 7427-7430; e). R. K. Pathak, S. Marrache, J. H. Choi, T. B. Berding, S. Dhar, The prodrug platin-A: simultaneous release of cisplatin and aspirin. **Angew. Chem. Int. Ed.** *2014*, 53, 1963-1967; f). S. G. Awuah, Y. R. Zheng, P. M. Bruno, M. T. Hemann, S. J. Lippard, A Pt(IV) Pro-drug Preferentially Targets Indoleamine-2,3-dioxygenase, Providing Enhanced Ovarian Cancer Immuno-Chemotherapy. **J. Am. Chem. Soc.** *2015*, 137, 14854-14857; g). J. Kasparkova, H. Kostrhunova, O. Novakova, R. Krˇikavov J. Vancˇo, Z.vn cˇek, V. Brabec, A Photoactivatable Platinum(IV) Complex Targeting Genomic DNA and Histone Deacetylases. **Angew. Chem. Int. Ed.** *2015*, 54, 14478-14482; h). R. Raveendran, J. P. Braude, E. Wexselblatt, V. Novohradsky, O. Stuchlikova, V. Brabec, V. Gandin, D. Gibson, Pt(iv) derivatives of cisplatin and oxaliplatin with phenylbutyrate axial ligands are potent cytotoxic agents that act by several mechanisms of action **Chem. Sci.** *2016*, 7, 2381-2391; i). G. Thiabaud, R. McCall, G. He, J. F. Arambula, Z. H. Siddik, J. L. Sessler, Activation of Platinum(IV) Prodrugs By Motexafin Gadolinium as a Redox Mediator. **Angew. Chem. Int. Ed.** *2016*, 55, 12626-12631; j). N. Muhammad, N. Sadia, C. Zhu, C. Luo, Z. Guo, X. Wang, Biotin-tagged platinum(iv) complexes as targeted cytostatic agents against breast cancer cells. **Chem. Commun.** *2017*, 53, 9971 – 9974; k). E. Petruzzella, J. P. Braude, J. R. AldrichWright, V. Gandin, D. Gibson, A Quadruple-Action Platinum(IV) Prodrug with Anticancer Activity Against KRAS Mutated Cancer Cell Lines. **Angew. Chem. Int. Ed.** *2017*, 56, 11539 – 11544; l). Ma L, Wang N, Ma R, Li C, Xu Z, Tse MK, Zhu G. Monochalcoplatin: An Actively Transported, Quickly Reducible, and Highly Potent PtIV Anticancer Prodrug. **Angew. Chem. Int. Ed.** *2018*, 57, 9098-9102. m). Petruzzella E, Sirota R, Solazzo I, Gandin V, Gibson D. Triple action Pt(iv) derivatives of cisplatin: a new class of potent anticancer agents that overcome resistance. **Chem Sci.** *2018*, 9, 4299-4307. n). Wang K, Zhu C, He Y, Zhang Z, Zhou W, Muhammad N, Guo Y, Wang X, Guo Z. Restraining cancer cells by dual metabolic inhibition with a mitochondrion-targeted platinum(II) complex. **Angew. Chem. Int. Ed.** *2019*, 58, 4638-4643; o). Zhu Z, Wang Z, Zhang C, Wang Y, Zhang H, Gan Z, Guo Z, Wang X. Mitochondrion-targeted platinum complexes suppressing lung cancer through multiple pathways involving energy metabolism. **Chem Sci.** *2019*, 10, 3089-3095; p). Babak MV, Zhi Y, Czarny B, Toh TB, Hooi L, Chow EK, Ang WH, Gibson D, Pastorin G. Dual-targeting dual-action platinum(IV) platform for enhanced anticancer activity and reduced nephrotoxicity**. Angew. Chem. Int. Ed.** *2019*, 58, 8109-8114. q). Chen F, Huang X, Wu M, Gou S, Hu W. A CK2-targeted Pt(IV) prodrug to disrupt DNA damage response. **Cancer Lett.** *2017*, 385, 168-178. r). Chun W, Ke-Jia W, Jin-Biao L, Xiao-Ming Z, Chung-Hang L and Dik-Lung M. A dual-functional molecular strategy for in situ suppressing and visualizing of neuraminidase in aqueous solution using iridium(iii) complexes. **Chem. Commun.**, *2019*, 55, 6353. s). Guan-Jun Y, Wanhe W, Simon Wing FM, Chun W, Betty Yuen KL, Xiang-Min M, Ke-Jia W, Hai-Jing Z, Chun-Yuen W, Vincent Kam W, DikLung M and Chung-Hang L. Selective inhibition of lysine-specific demethylase 5A (KDM5A) using a rhodium(III) complex for triple-negative breast cancer therapy. **Angew. Chem. Int. Ed.** *2018*, 57, 13091. t). Huaiyi H, Samya B, Kangqiang Q, Pingyu Z, Olivier B, Thomas M, Martin J. P, Guy J. C, Michael S, Vasilios G. S, Gilles G, Hui C and Peter J. S. Targeted photoredox catalysis in cancer cells. **Nat. Chem.**, *2019*, DOI: 10.1038/s41557-019-0328-4.

[9] a) Banerjee, S.; Veale, E. B.; Phelan, C. M.; Murphy, S. A.; Tocci, G.M.; Gillespie, L. J.; Frimannsson, D. O.; Kelly, J. M.; Gunnlaugsson, T. Recent advances in the development of 1,8-naphthalimide based DNA targeting binders, anticancer and fluorescent cellular imaging agents. **Chem. Soc. Rev.** 2013,

42, 1601−1618. b) Chen, Z.; Han, L.; Xu, M.; Xu, Y.; Qian, X. Rationally designed multitarget anticancer agents. **Curr. Med. Chem**. 2013, 20, 1694−1714. c) Seifert, S.; Shoyama, K.; Schmidt, D.; Wurthner, F. An electronpoor C64 nanographene by palladium-catalyzed cascade c-c bond formation: one-pot synthesis and single-crystal structure analysis. **Angew. Chem., Int. Ed.** 2016, 55, 6390−6395.

[10] a) Chua, E.Y., Davey, G.E., Chin, C.F., Dröge, P., Ang, W.H., Davey, C.A., Stereochemical control of nucleosome targeting by platinum-intercalator antitumor agents. **Nucleic Acids Res.** 2015, 43, 5285–5296. b) Herrera, J.M., Mendes, F., Gama, S., Santos, I., Navarro-Ranninger, C., Cabrera, S., Quiroga, A.G., Design and biological evaluation of new platinum(II) complexes bearing ligands with DNA-targeting ability. **Inorg. Chem.** 2014, 53, 12627–12634. c) Navas, F., Mendes, F., Santos, I., Navarro-Ranninger, C., Cabrera, S., Quiroga, A.G., Enhanced cytotoxicity and reactivity of a novel platinum(IV) family with DNA–targeting naphthalimide ligands. **Inorg. Chem.** 2017, 56, 6175–6183; d) Oliveira, K.N., Andermark, V., Onambele, L.A., Organotin complexes containing carboxylate ligands with maleimide and naphthalimide derived partial structures: TrxR inhibition, cytotoxicity and activity in resistant cancer cells. **Eur. J. Med. Chem.** 2014, 87, 794–800.

[11] a). Li, M.; Li, Q.; Zhang, Y. H.; Tian, Z. Y.; Ma, H. X.; Zhao, J.; Xie, S. Q.; Wang, C. J. Antitumor effects and preliminary systemic toxicity of ANISpm in vivo and in vitro. **Anti-Cancer Drugs** 2013, 24, 32−42. b). Wang, Y. X.; Zhang, X.; Zhao, J.; Xie, S. Q.; Wang, C. J. Nonhematotoxic naphthalene diimide modified by polyamine: synthesis and biological evaluation. **J. Med. Chem.** 2012, 55, 3502−3512. c). Dai, F. J.; Li, Q.; Wang, Y. X.; Ge, C. C.; Feng, C.; Xie, S. Q.; He, H.; Xu, X.; Wang, C. J. Design, Synthesis, and Biological Evaluation of Mitochondria-Targeted Flavone-Naphthalimide-Polyamine Conjugates with Antimetastatic Activity. **J. Med. Chem.** 2017, 60, 2071−2083. d). Li J, Tian R, Ge C, Chen Y, Liu X, Wang Y, Yang Y, Luo W, Dai F, Wang S, Chen S, Xie S, Wang C. Discovery of the Polyamine Conjugate with Benzo[cd]indol-2(1 H)-one as a Lysosome-Targeted Antimetastatic Agent. **J Med Chem.** 2018, 61, 6814-6829. e). Li, Q.; Zhai, Y.; Luo, W.; Zhu, Z.; Zhang, X.; Xie, S.; Hong, C.; Wang, Y.; Su, Y.; Zhao, J.; Wang, C. Synthesis and biological properties of polyamine modified flavonoids as hepatocellular carcinoma inhibitors. **Eur. J. Med. Chem.** 2016, 121, 110 −119. f). Chaojie, W.; Jean-Guy, D.; Laura, C.; Fanta, K.; Horacio, C.; John, B.; Richard Andrew, G.; Otto, P IV. Defining the molecular requirements for the selective delivery of polyamine conjugates into cells containing active polyamine transporters. **J Med Chem.** 2003, 46, 5129-5138. g). Chaojie, W.; Jean-Guy, D.; John, B.; Otto P IV. Molecular requirements for targeting the polyamine transport system. Synthesis and biological evaluation of polyamine-anthracene conjugates. **J Med Chem.** 2003, 46, 2672-2682. h). Chaojie, W.; Jean-Guy, D.; John, B.; Otto, P IV. Synthesis and biological evaluation of N1-(anthracen-9-ylmethyl)triamines as molecular recognition elements for the polyamine transporter. **J Med Chem.** 2003, 46, 2663-2671. i). Xie, S.; Wang, J.; Zhang, Y.; Wang, C. Antitumor conjugates with polyamine vectors and their molecular mechanisms. **Expert Opin Drug Deliv.** 2010, 7, 1049-1061. j). Cong W, Ping R, Ying Z, Xiaomin L, Jun W, Xiaoxiao W, Tong L, Shasha W, Jiuzhou H, Wei L, Qian L, Jinghua L, Fujun D, Dong F, Chaojie W, Songqiang X. Spermidine/spermine N1-acetyltransferase regulates cell growth and metastasis via AKT/β-catenin signaling pathways in hepatocellular and colorectal carcinoma cells. **Oncotarget**, *2017*, 8, 1092-1109.

[12] a). Forner, A.; Llovet, J. M.; Bruix, J. Hepatocellular carcinoma. **Lancet** 2012, 379, 1245−1255; b). Dou, C.; Liu, Z.; Xu, M.; Jia, Y.; Wang, Y.; Li, Q.; Yang, W.; Zheng, X.; Tu, K.; Liu, Q. miR-187-3p inhibits the metastasis and epithelial-mesenchymal transition of hepatocellular carcinoma by targeting S100A4. **Cancer Lett.** 2016, 381, 380−390; c). Valastyan, S.; Weinberg, R. A. Tumor metastasis: molecular insights and evolving paradigms. **Cell** 2011, 147, 275−292; d). Sonnenschein, C.; Soto, A. M. Cancer Metastases: So Close and So Far. **J. Natl. Cancer Inst.** 2015, 107, djv236; e). Ran, S. The Role of TLR4 in Chemotherapy-Driven Metastasis. **Cancer Res.** 2015, 75, 2405−2410. f) Wang, P., Du, Y., Zhao, X., Miao, Y., Song, C. P. The MPK6-ERF6-ROSresponsive cis-acting Element7/GCC box complex modulates oxidative gene
transcription and the oxidative response in Arabidopsis. **Plant Physiol.** 2013, 161, 1392–1408.

[13] a) W. M. Bonner, C. E. Redon, J. S. Dickey, A. J. Nakamura, O. A. Sedelnikova, S. Solier, Y. Pommier, GammaH2AX and cancer. **Nat. Rev. Cancer** 2008, 8, 957 – 967; b) Dai, Y. J., Hui, K. M., Zhang, Y. H., Liu, Y., Wang, Y. Q., Zhao, L. J., et al. Three STATs are involved in the regulation of the expression of antimicrobial peptides in the triangle sail mussel, Hyriopsis cumingii. **Fish Shellfish Immunol.** 2017, 63, 181–188.

[14] a) Vequaud, E.; Desplanques, G.; Je ze quel, P.; Juin, P.; Barille -Nion, S. Survivin contributes to DNA repair by homologous recombination in breast cancer cells. **Breast Cancer Res. Treat.** 2016, 155, 53-63. b) A. R. Mattoo, R. K. Pandita, S. Chakraborty, V. Charaka, K. Mujoo, C. R. Hunt and T. K. Pandita, MCL-1 Depletion Impairs DNA Double-Strand Break Repair and Reinitiation of Stalled DNA Replication Forks. **Mol. Cell. Biol.**, 2017, 37, e00535-16. c) J. Her and S. F. Bunting, How Cells Ensure Correct Repair of DNA Double-Strand Breaks. **J. Biol. Chem.**, 2018, 293, 10502–10511. d) A. J. Deans and S. C. West, DNA Interstrand Crosslink Repair and Cancer. **Nat. Rev. Cancer**, 2011, 11, 467–480.

[15] a) Hengel, S. R.; Spies, M. A.; Spies, M. Small-molecule inhibitors targeting DNA repair and DNA repair deficiency in research and cancer therapy. **Cell Chem. Biol.** 2017, 24, 1101-1119. b) Huang, F.; Mazina, O. M.; Zentner, I. J.; Cocklin, S.; Mazin, A. V. Inhibition ofhomologous recombination in human cells by targeting RAD51 recombinase. **J. Med. Chem.** 2012, 55, 3011-3020. c) Chen, S. J.; Liu, R. X.; Wang, Q.; Qi, Z. H.; Hu, Y. C.; Zhou, P. K.; Wang, Z. D. MiR-34s

negatively regulate homologous recombination through targeting RAD51. **Arch. Biochem. Biophys.** 2019, 666, 73-82.
d) Chen, M., Li, K., Li, H., Song, C. P., and Miao, Y. The glutathione peroxidase gene family in gossypium hirsutum: genome-wide identification, classification, gene expression and functional analysis. **Sci. Rep.** 2017, 7, 44743.

Table of Contents Graphic

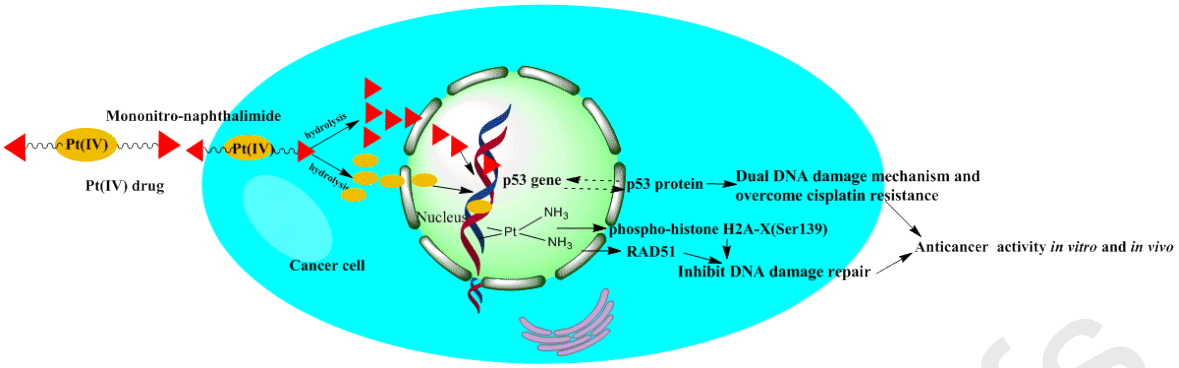

Highlights

1．Mononitro-naphthalimide Pt(IV) complex **10b** targeting DNA damage response *via* a dual-DNA-damage approach to overcome cisplatin resistance.

2. **10b** targets resistant cells in a totally different way from the existing Pt drugs.

3．The highest fold increase (FI) for A549cisR cells and the lowest for A549 indicated **10b** preferentially accumulated in resistant cell lines.

Dear Editor:

We would like to submit the enclosed manuscript entitled " A Pt(IV)-based Mononitro-naphthalimide Conjugate with Minimized Side-effects Targeting DNA Damage Response via a Dual-DNA-Damage Approach to Overcome Cisplatin Resistance" and manuscript is approved by all authors for publication. I would like to declare on behalf of my co-authors that this work has not been published previously, and not under consideration for publication elsewhere, in whole or in part. All the authors listed have approved the manuscript that is enclosed.

The authors Jing Ma, and Songqiang Xie, contribute to the conception, design, analysis and writing of the study against the collection of data and other routine work. Hanfang Liu, Yingguang Li, Linrong Li, Kexin Yue, contribute to the synthesis of compounds in this paper. And Jie Niu contribute to the mechanism research and animal experiments *in vitro* and *in vivo*.

Hopefully we have addressed all of your concerns.

Best wishes.

Your sincerely,

Dr. Jing Ma

Institute of Chemical Biology, College of Pharmacy, Henan University, Kaifeng, 475004, China. E-mail: majing.1988.ok@163.com

Prof. Dr. Songqiang Xie

Institute of Chemical Biology, College of Pharmacy, Henan University, Kaifeng, 475004, China. E-mail: xiesq@vip.henu.edu.cn

Thanks very much for your attention.

Sincerely yours,

All authors